

A surface plasmon enhanced FLIM-FRET imaging approach based on Au nanoparticles

Yinan Zhang^{1*}, Yu Chen², Jun Yu³ and David JS Birch²

¹College of Physic, Jilin University, 2699 Qianjin Street, Changchun, Jilin Province, 130012, China PR

²Photophysics Group, Department of Physics, SUPA, University of Strathclyde, 107 Rottenrow, Glasgow G4 0NG, UK

³Strathclyde Institute of Pharmacy and Biomedical Sciences, 204 George Street, Glasgow G1 1XW, UK

Abstract

In this report we have demonstrated a fluorescence resonant energy transfer (FRET)-fluorescence lifetime imaging microscopy (FLIM) combined approach to study the intracellular pathway of gold nanoparticles. The detected energy transfer between gold nanorods (GNRs) and green fluorescence protein (GFP) labeled Hela cell early endosomes and the in-depth lifetime distribution analysis on the transfer process suggest an endocytotic uptake process of GNRs. Furthermore, the FRET-FLIM method profits from a surface plasmon enhanced energy transfer mechanism when taking into consideration of GNRs and two photon excitation, and is effective in biological imaging, sensing, and even in single molecular tracing in both *in vivo* and *in vitro* studies.

Introduction

Due to their unique physical and chemical properties, gold nanoparticles have been widely applied in *in vivo* and *in vitro* biological research, such as drug delivery [1-5], cancer therapy [6-13], imaging and sensing [14-20]. Therefore, understanding the intracellular pathways of gold nanoparticles and uptake mechanism is essential for all these applications, as these studies will provide information on uptake rate, route, final intracellular location, and the effects of nanoparticles to cell organelles, etc. However, this is not a straightforward task, because the properties of cells, such as cell groups and types, and characteristics of nanoparticles, such as the size, shape, surface charge and coating conditions, will all play a role effects on the uptake process [21-28]. There are a variety of nanoparticle pathways and mechanisms into cell membrane, and results between different publications are still inconsistent [29-37]. Nowadays traditional research methodologies to track locations of nanoparticles in cell cultures all have their own advantages, as well as drawbacks. For example, traditional fluorescence microscopy can be operated *in vivo* or *in vitro*, and can be applied with cell organelles stained with a variety of fluorescent probes, but is lack of high sensitivity and resolution. Sometimes it is difficult to conclude if the overlapping pixel is real co-localization or just structures in close approximation [38,39]. While electron microscopes, such as transmission electron microscopy (TEM), can provide higher spatial resolution, but the specimen has to be treated at vacuum, therefore is not possible to provide *in situ*, time lapse examination [40,41].

Here we introduce a two-photon fluorescence lifetime imaging microscopy (FLIM) method monitoring the Foster resonance energy transfer (FRET) effect between gold nanorods (GNRs) particles and fluorescent molecules to study the uptake mechanism of GNRs. As the FRET effect will only be triggered in several nanometers' range, it is a very sensitive distance measurement, or 'the spectroscopic ruler'. Therefore FLIM-FRET method can directly indicate if the gold particles are enclosed in specific cellular vesicles, such as the endosomes, and can be applied *in vivo* and *in vitro*.

In the first part of this manuscript, we will demonstrate the enhanced energy transfer effect between GNRs and fluorophores under two photon excitation; in the second part we will study if early endosomes are involved in the intracellular process of GNRs, by staining the vesicles with green fluorescence protein (GFP) and monitoring FRET with FLIM.

Materials and methods

Gold nanorods were synthesized by seeded growth method. Multi-layer coated nanoparticles were prepared following a layer by layer procedure: capped nanorods were centrifuged at 8500 rpm for 10 minutes, and were modified to optical density (O.D.) 1.0; then nanorods solution was mixed with polystyrenesulfonate (PSS) solution (10mg/ml in NaCl) with volume 5:1 and stirred for 5 minutes; after centrifuged at 8500 rpm for 15 minutes to remove excess polymers, and the remaining PSS coated nanorods solution was modified to O.D. 1.0; then PSS coated particles were mixed with poly-diallyldimethylammonium chloride (PDDAC) solution (10mg/ml in NaCl) with volume ratio 5:1 and stirred for another 5 minutes; excess polymers can be removed by centrifuge. Multi-layer PSS/PDDAC coated nanoparticles can be prepared by repeating the process described above. The detailed recipe can be found at [42].

Alexa Fluor405 dyes were purchased from Sigma-Aldrich. 'Sample F0-1' was mixed with 500µl gold nanorods and 150µl F405dye, and 'Sample F0-2' was mixture solution of 500µl gold nanorods and 300µl F405dye.

Correspondence to: Yinan Zhang, Lecturer, College of Physic, Jilin University, 2699 Qianjin Street, Changchun, Jilin Province, 130012 China PR, Tel: 0086-186-2672-6704; Email: zhangyinan@jlu.edu.cn

Key words: cell imaging, fluorescence resonance energy transfer, gold nanoparticles, optical imaging and microscopy

Received: May 08, 2017; **Accepted:** May 24, 2017; **Published:** May 29, 2017

Hela cell-lines were obtained from American Type Culture Collection. Cell culture medium was high-glucose (4.5 g/l) DMEM containing foetal calf serum (10%), L-glutamine (2.9mg/mL), antibiotic-antimycotic solution (GIBCO). Cells were routinely cultured at 37°C under 5% CO₂. Celllight Endosomes-GFP BacMam 2.0 GFP early endosome marker was purchased from Invitrogen and applied following manual instruction.

Fluorescence decay times were obtained using both HORIBA-IBH TCSPC lifetime measurement kit and B&H module. Fluorescence and FLIM images were taken with Zeiss LSM-510 confocal microscope and attached B&H module. Single photon lifetime measurements were excited by 374nm laser, and the emission light was collected at 405 nm. For the two-photon excitation lifetime measurement, all mixture solutions were placed in an imaging chamber and excited by a chameleon pulse laser operated at 810nm. The emission light was collected through a 390-465 nm bandpass filter and the decay time was measured with B&H FLIM module operating at 'single' mode.

Results and discussion

Surface plasmon enhanced energy transfer effect

We have examined the interaction between gold nanoparticles and Fluor405 dyes in solution phase by monitoring the fluorescence lifetime change. Under both single and two photon excitation, the decay times of mixture solutions are found to decrease compared to that of pure reference dye solution, indicating energy transfer has occurred. After fitting all decay curves with multi-exponential model

$$I = I_0 \sum_{i=1}^n B_i \exp(-t / T_i) \quad (1)$$

The difference between samples can be demonstrated in a quantitative manner. In this case, for F0-1 and F0-2 $n=3$, and for F405 $n=2$. The fitting results can be found in Tables 1 and 2, with χ^2 indicating the goodness of fitting.

As shown in Tables 1 and 2, under single photon excitation, decay time of F405 can be well fitted by a two-exponential model, and the dominating long lifetime component is around 3.6ns. When mixed with gold nanorods, the longer component drops to 3.26 ns for sample F0-1 and 3.15ns for sample F0-2. As F0-1 has a shorter distance between donor and acceptor than F0-2, the result shows less decrease in decay time. In the two-photon excitation experiments, the decay curves can be fitted by a two-exponential model, in which the shorter component is from gold nanorods and the longer one from Fluor405. Table 2 shows a more significant decrease in lifetime (from 3.85ns down to around 2.8 and 2.6ns), which may suggest an enhanced energy transfer process under two-photon excitation. Similar to what has been observed from hybrid system of DAPI and gold nanorods [38] this two-photon induced enhancement effect cannot be explained by Förster resonance energy transfer or surface energy transfer model, because both theories do not consider the effect from excitation conditions. It has been revealed that in the vicinity of metal particles or surfaces, the radiative dipole of donor fluorophores interacts with both the incidence and scattered electromagnetic field. Therefore we attribute the enhanced energy transfer under two-photon excitation to the effect arising from localized longitudinal surface plasmon oscillation, which resonates at the incidence wavelength and enhances the non-radiative energy transfer decay rate from the donor fluorophores to the nanoparticles.

Moreover, no change in lifetime has been found in the mixture solution of gold nanospheres and Fluor405, no matter single or two-photon excitation. This is consistent with the result obtained from DAPI-gold nanorods system [38].

FLIM-FRET imaging: research on cell uptake mechanism of gold nanoparticles

Figure 1(a) is a typical confocal image of Hela cells with early endosome labeled by GFP. Figure 1(b) shows the control sample where Hela cells were not treated with GFP and examined under the same imaging configuration. Compared to labeled ones, where bright spots in the image are considered to be fluorescence from GFP, no strong fluorescence signal but only weak cell autofluorescence can be seen in Figure 1(b). In Figure 1 (c) and (d), the same imaging region is examined under two-photon excitation. Figure 1(c) is the two-photon luminescence (TPL) intensity image taken from the same sample as in Figure 1(a) excited under 850nm femto-second laser and 500-550nm emission bandpass filter. Figure 1(d) is the FLIM image of Figure 1(c), where different colors in each image pixel varying from orange to blue demonstrate different fluorescence lifetimes ranging from 0 to 3ns. The fluorescence lifetime was obtained by fitting the experimental decay curves by a single exponential decay model, as shown in Figure 1(e). Lifetime of GFP in cell culture is found to be around 2ns, as seen in the lifetime distribution in Figure 1(f). This lifetime value is in consistent with published results [43, 44]. By comparing the images shown in Figure 1, we can confirm that early endosomes in Hela cells have been well stained by GFP. GFP emit strong and stable fluorescence under both single and two-photon excitation.

To investigate the uptake process of gold nanorods by Hela cells, we have incubated the cells with gold nanorods at 5% volume concentration under 37°C for different time periods, from 30 minutes to 1 hour. FLIM images are shown in Figure 2: from (a) to (c), the gold nanorods incubation time is 30minutes, 45 minutes, and 1 hour respectively. Decay curves of all pixels in images have been fitted by a two-exponential model (equ.1, $n=2$) as the luminescence from gold nanorods has to be considered. The coded color hereby represents the average lifetime τ_{ave} , which can be expressed by

$$\tau_{ave} = \sum_i^n B_i T_i \quad (2)$$

In the FLIM images, green/blue pixels are emission from GFP, while brighter orange/yellow spots in cells are considered to be signals from gold nanorods or overlapping areas where both emissions from GNRs and GFP were found. This is because that the decay time scale of TPL from GNRs is extremely small (in system response level), while the intensity is much stronger than that from GFP (contribution over 80% of total signals). Therefore even the lifetime of GFP is as long as 2ns, the average lifetimes in these pixels are quite short, usually around several hundred pico seconds.

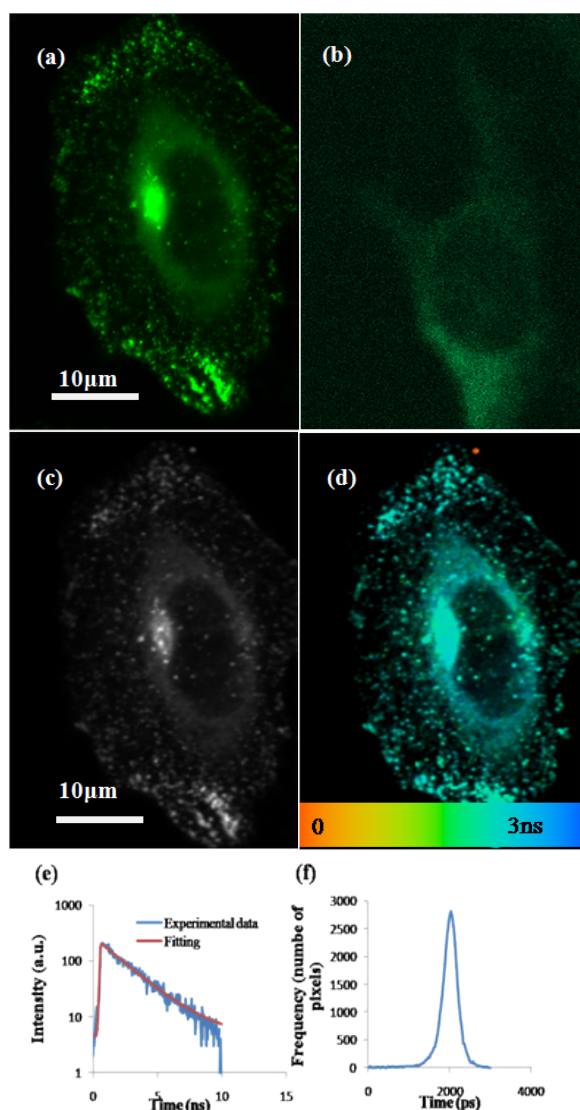
A few gold nanorods were found in cells after incubation of 30min and 45min, while significant amount of nanorods have been found in cells after 1 hour incubation, demonstrated by the increasing in number of the pixels displaying shorter lifetime, or orange color as shown in figure 2 (a) - (c). To investigate the influence from surface functionality of nanoparticle on cell up taking, we treated Hela cells with multi-layer coated gold nanorods. The result of 4 layer coated nanorods with ending layer PDDAC is shown in Figure 2(e). From the image, a higher particle concentration internalized by Hela cells has been found, which suggest polymer coated gold nanorods are easier to go through the cell membrane compared to CTAB capped ones. This is in consistent with our previous research on cytotoxicity of GNRs, where cells treated with

Table 1. Fitting results of mixture solution and pure Fluor405 dye under single photon excitation. A multi-exponential decay model described as equ.1 was applied. For F0-1 and F0-2 $n=3$ and for F405 control $n=2$.

	B1	B2	B3	T1	T2	T3	χ^2
F0-1	23.2%	2.64%	74.16%	$1.57 \pm 0.06\text{ns}$	$0.27 \pm 0.02\text{ns}$	$3.26 \pm 0.08\text{ns}$	1.11
F0-2	32.5%	3.25%	64.25%	$1.84 \pm 0.09\text{ns}$	$0.38 \pm 0.02\text{ns}$	$3.15 \pm 0.01\text{ns}$	1.02
F405 control	4.76%	95.24%	N/A	$0.27 \pm 0.05\text{ns}$	$3.60 \pm 0.03\text{ns}$	N/A	1.03

Table 2. Fitting results of two-photon excitation data. A multi-exponential decay model described as equ. 1 was applied. For F0-1 and F0-2 $n=2$ and for F405 control $n=1$.

	B1	B2	T1	T2	χ^2
F0-1	4.88%	95.12%	$2.81 \pm 0.02\text{ns}$	$0.0090 \pm 0.0002\text{ns}$	1.09
F0-2	3.05%	96.94%	$2.59 \pm 0.01\text{ns}$	$0.0062 \pm 0.0002\text{ns}$	0.86
F405 control	100%	N/A	$3.75 \pm 0.01\text{ns}$	N/A	1.04

**Figure 1.** (a) Confocal fluorescence image of GFP stained HeLa cells, excited under 488nm, emission collected with longpass 505nm filter; (b) HeLa cells without GFP labeling; (c), (d) Intensity and FLIM image of two-photon excited GFP stained HeLa cells, excited under 850nm and emission collected with 500-550nm bandpass filter. For FLIM image, the lifetime ranges from 0 (orange) to 3ns (blue); (e) Typical decay curve of fluorescence from GFP in cell culture; (f) Distribution of fluorescence lifetimes displayed in (d).

polymer coated GNRs showed a higher survival rate. In contrast to intensity image, Figure 2(d), which cannot clearly distinguish between luminescence from gold particles and GFP, FLIM provides a more

sensitive and convenient method for monitoring cell uptake process, with a potential for in vitro live cell monitoring.

Although all bright spots in FLIM images are found to be overlapping pixels, which means that GNRs overlaps with GFP stained early endosomes and there are no isolating GNRs, a further analysis on FLIM results has been carried out to study the FRET between gold particles and GFP labeled endosomes in turn to confirm the endocytic pathway. By examining the longer component, which is supposed to be the contribution from GFP at the overlapping areas, we can determine if there was energy transfer between GFP and gold nanoparticles when they were close enough to each other. Shorter lifetimes of GFP (even down to around 1ns) do exist where gold nanorods were present, but as shown in Figure 1(f), lifetime distribution of GFP in FLIM experiments ranges from 1.5ns to 2.5ns. To clarify whether the short lifetime is due to normal lifetime distribution or specific mechanism, we used a statistical approach to compare the lifetime change. As shown in Figure 2(f), the longer component (lifetime of GFP) subtracted from 58 overlapping pixels in different FLIM images have been sorted in 100 ps interval from 1100 ps to 2400 ps. Compared to a symmetric lifetime distribution of GFP in Figure 1. (f), lifetime values of GFP in the vicinity of gold nanorods form an asymmetric distribution, with a higher rate of shorter lifetime than the longer one and a long tail reaching 1.1ns, which suggests energy transfer process does exist between GFP and gold nanorods. Considering the size of early endosomes is around several hundred nm, and energy transfer only occurs when donor and acceptor fluorophores are in a near vicinity (within 8nm for Förster resonance energy transfer and double the distance for surface energy transfer), this may explains why only some of the GNRs close enough to GFP label sites demonstrated FRET effect. This result benefits from the two-photon enhanced FRET, which makes the FLIM method more sensitive when tracing GNRs. There are more than one endocytic mechanisms on nanoparticle-intracellular uptake, such as Clathrin dependent/independent or Dynamin dependent/independent pathways. And each involves a variety of vesicles, early endosomes, phagosomes, macropinosomes, late endosomes, lysosomes for instance [45-50]. We have demonstrated that GNRs follow an endocytosis uptake mechanism and early endosomes are involved, with a time dependent manner.

Conclusions

In this report, we first investigated the influence of excitation conditions on the energy transfer process in fluorophores-gold nanoparticle hybrid systems. An enhanced energy transfer has been detected under two-photon excitation, where the incidence excitation frequency resonates with the longitudinal surface plasmon band of gold nanorods and enhances the non-radiative energy transfer rate from donor to acceptor particles. Then based on the two-photon enhanced FRET method, we studied the intracellular pathways of gold nanorods. A endocytic pathway with early endosomes taking part has been confirmed. After incubated for 1hr, the uptake number of GNRs by HeLa cells increases dramatically. Polymer coating on GNRs surface do promotes the uptake rate. Moreover, by staining the specific endocytic vesicles, FLIM-FRET combined with gold nanoparticles, especially

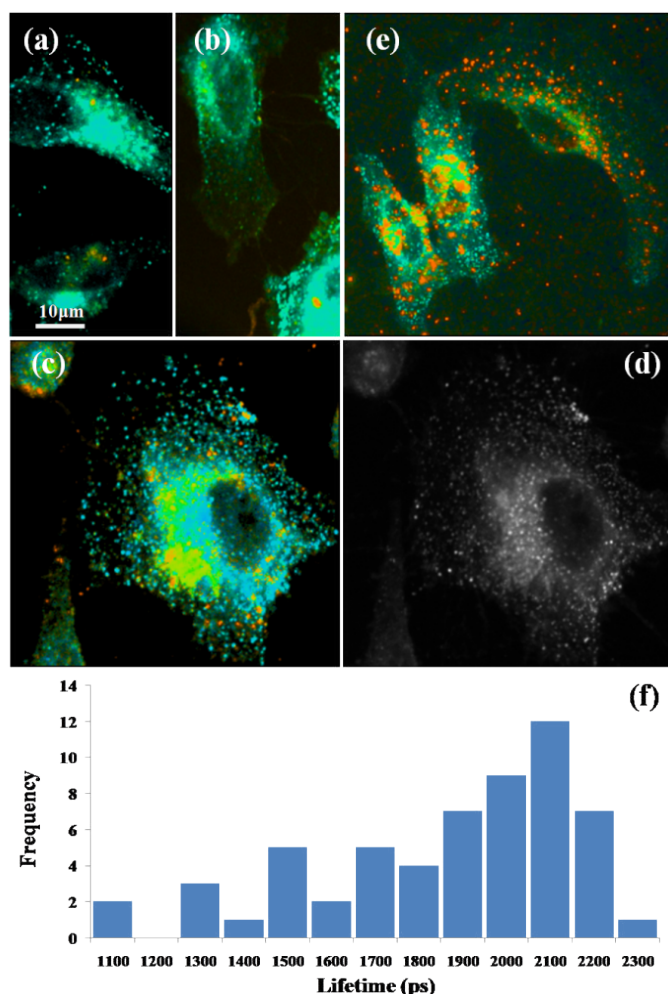


Figure 2. FLIM images of GFP-stained HeLa cells incubated with CTAB capped gold nanorods for (a) 30 minutes, (b) 45 minutes, and (c) 1 hour; (d) intensity image of 1 hour sample; (e) incubated with multi-layer coated gold nanorods for 1 hour; (f) Lifetime distribution of GFP in overlapping areas.

GNRs, can be a highly sensitive tracing technique for uptake study and further biological research.

Conflict of interest

We have no conflict of interests.

References

- Alkilany AM, Thompson LB, Boulos SP, Sisco PN, Murphy CJ (2012) Gold nanorods: Their potential for photothermal therapeutics and drug delivery, tempered by the complexity of their biological interactions. *Adv Drug Deliv Rev* 64: 190-199. [\[Crossref\]](#)
- Biju V (2014) Chemical modifications and bioconjugate reactions of nanomaterials for sensing, imaging, drug delivery and therapy. *Chem Soc Rev* 43: 744-764. [\[Crossref\]](#)
- Chou LYT, Zagorovsky K, Chan WCW (2014) DNA assembly of nanoparticle superstructures for controlled biological delivery and elimination. *Nat Nanotechnol* 9: 148-155
- Ghosh P, Han G, De M, Kim CK, Rotello VM (2008) Gold nanoparticles in delivery applications. *Adv Drug Deliv Rev* 60: 1307-1315. [\[Crossref\]](#)
- Torchilin VP (2014) Multifunctional stimuli-sensitive nanoparticulate systems for drug delivery. *Nat Rev Drug Discov* 13: 813-827.
- Cheng L, Wang C, Feng L, Yang K, Liu Z (2014) Functional nanomaterials for phototherapies of cancer. *Chem Rev* 114: 10869-10939. [\[Crossref\]](#)
- Guo YJ, Sun GM, Zhang L, Tang YJ, Luo JJ, et al., (2014) Multifunctional optical probe based on gold nanorods for detection and identification of cancer cells. *Sens and Actuators B-Chemical* 191: 741-749.
- Huang XH, El-Sayed IH, Qian W, El-Sayed MA (2006) Cancer cell imaging and photothermal therapy in the near-infrared region by using gold nanorods. *J Am Chem Soc* 128: 2115-2120.
- Vigderman L, Manna P, Zubarev ER (2012) Quantitative Replacement of Cetyl Trimethylammonium Bromide by Cationic Thiol Ligands on the Surface of Gold Nanorods and Their Extremely Large Uptake by Cancer Cells. *Angew Chem Int Ed Engl* 51: 636-641. [\[Crossref\]](#)
- Wang B, Wang JH, Liu Q, Huang H, Chen M, et al., (2014) Rose-bengal-conjugated gold nanorods for in vivo photodynamic and photothermal oral cancer therapies. *Biomaterials* 35: 1954-1966. [\[Crossref\]](#)
- Xu Y, Wang J, Li X, Liu Y, Dai L, et al., (2014) Selective inhibition of breast cancer stem cells by gold nanorods mediated plasmonic hyperthermia. *Biomaterials* 35: 4667-4677. [\[Crossref\]](#)
- Zhang ZJ, Wang LM, Wang J, Jiang XM, Li XH, et al., (2012) Mesoporous Silica-Coated Gold Nanorods as a Light-Mediated Multifunctional Theranostic Platform for Cancer Treatment. *Adv Mater* 24: 1418-1423. [\[Crossref\]](#)
- Ando J, Fujita K, Smith NI, Kawata S (2011) Dynamic SERS Imaging of Cellular Transport Pathways with Endocytosed Gold Nanoparticles. *Nano Letters* 11: 5344-5348. [\[Crossref\]](#)
- Boisselier E, Astruc D (2009) Gold nanoparticles in nanomedicine: preparations, imaging, diagnostics, therapies and toxicity. *Chem Soc Rev* 38: 1759-1782. [\[Crossref\]](#)
- Tong L, Wei QS, Wei A, Cheng JX (2009) Gold Nanorods as Contrast Agents for Biological Imaging: Optical Properties, Surface Conjugation and Photothermal Effects. *Photochem Photobiol* 85: 21-32. [\[Crossref\]](#)
- Jain PK, Huang X, El-Sayed IH, El-Sayed MA (2008) Nobel Metals on the Nanoscale: Optical and Photothermal Properties and Some Applications in Imaging, Sensing, Biology, and Medicine. *Acc Chem Res* 41: 1578-1586. [\[Crossref\]](#)
- Giljohann DA, Seferos DS, Daniel WL, Massich MD, Patel PC, et al., (2010) Gold nanoparticles for biology and medicine. *Angew Chem Int Ed Engl* 49: 3280-3294. [\[Crossref\]](#)
- Kneipp J, Kneipp H, McLaughlin M, Brown D, Kneipp K (2006) In vivo molecular probing of cellular compartments with gold nanoparticles and nanoaggregates. *Nano Lett* 6: 2225-2231. [\[Crossref\]](#)
- Li N, Zhao PX, Astruc D (2014) Anisotropic Gold Nanoparticles: Synthesis, Properties, Applications, and Toxicity. *Angew Chem Int Ed Engl* 53: 1756-1789. [\[Crossref\]](#)
- Zhang ZJ, Wang J, Nie JX, Wen T, Ji YL, et al., (2014) Near Infrared Laser-Induced Targeted Cancer Therapy Using Thermoresponsive Polymer Encapsulated Gold Nanorods. *J Am Chem Soc* 136: 7317-7326. [\[Crossref\]](#)
- Alkilany AM, Nagaria PK, Hexel CR, Shaw TJ, Murphy CJ, et al., (2009) Cellular Uptake and Cytotoxicity of Gold Nanorods: Molecular Origin of Cytotoxicity and Surface Effects. *Small* 5: 701-708.
- Brandenberger C, Muehlfeld C, Ali Z, Lenz AG, Schmid O, et al., (2010) Quantitative Evaluation of Cellular Uptake and Trafficking of Plain and Polyethylene Glycol-Coated Gold Nanoparticles. *Small* 6: 1669-1678. [\[Crossref\]](#)
- Chithrani BD, Chan WC (2007) Elucidating the mechanism of cellular uptake and removal of protein-coated gold nanoparticles of different sizes and shapes. *Nano Lett* 7: 1542-1550. [\[Crossref\]](#)
- Huff TB1, Hansen MN, Zhao Y, Cheng JX, Wei A (2007) Controlling the cellular uptake of gold nanorods. *Langmuir* 23: 1596-1599. [\[Crossref\]](#)
- Ma X, Wu Y, Jin S, Tian Y, Zhang X, et al., (2011) Gold Nanoparticles Induce Autophagosome Accumulation through Size-Dependent Nanoparticle Uptake and Lysosome Impairment. *ACS Nano* 5: 8629-8639.
- Patel PC, Giljohann DA, Daniel WL, Zheng D, Prigodich AE, et al., (2010) Scavenger Receptors Mediate Cellular Uptake of Polyvalent Oligonucleotide-Functionalized Gold Nanoparticles. *Bioconjug Chem* 21: 2250-2256.
- Zhu XM, Fang C, Jia H, Huang Y, Cheng CHK, et al., (2014) Cellular uptake behaviour, photothermal therapy performance, and cytotoxicity of gold nanorods with various coatings. *Nanoscale* 6: 11462-11472. [\[Crossref\]](#)
- Yi C, Liu D, Fong CC, Zhang J, Yang M, (2014) Gold Nanoparticles Promote Osteogenic Differentiation of Mesenchymal Stem Cells through p38 MAPK Pathway. *ACS Nano* 4: 6439-6448. [\[Crossref\]](#)

29. Haiss W, Thanh NT, Aveyard J, Fernig DG (2007) Determination of size and concentration of gold nanoparticles from UV-vis spectra. *Anal Chem* 79: 4215-4221. [[Crossref](#)]
30. Oh N, Park JH (2014) Endocytosis and exocytosis of nanoparticles in mammalian cells. *Int J Nanomedicine* 9 Suppl 1: 51-63. [[Crossref](#)]
31. Shukla R, Bansal V, Chaudhary M, Basu A, Bhonde RR, et al., (2005) Biocompatibility of gold nanoparticles and their endocytotic fate inside the cellular compartment: A microscopic overview. *Langmuir* 21: 10644-10654. [[Crossref](#)]
32. Yen HJ, Hsu SH, Tsai CL (2009) Cytotoxicity and Immunological Response of Gold and Silver Nanoparticles of Different Sizes. *Small* 5: 1553-1561. [[Crossref](#)]
33. Nativo P, Prior IA, Brust M (2008) Uptake and intracellular fate of surface-modified gold nanoparticles. *ACS Nano* 2: 1639-1644. [[Crossref](#)]
34. Zhang W, Ji Y, Wu X, Xu H (2013) Trafficking of Gold Nanorods in Breast Cancer Cells: Uptake, Lysosome Maturation, and Elimination. *ACS Appl Mater Interfaces* 5: 9856-9865. [[Crossref](#)]
35. Zhang S, Li J, Lykotrafitis G, Bao G, Suresh S (2009) Size-Dependent Endocytosis of Nanoparticles. *Adv Mater* 21: 419-424. [[Crossref](#)]
36. Stark WJ (2011) Nanoparticles in Biological System. *Angew Chem Int Ed* 50: 1242-1258. [[Crossref](#)]
37. Zhang Y, Birch DJS, Chen Y, (2011) Two-photon excited surface Plasmon enhanced energy transfer between DPAI and gold nanoparticles: Opportunities in intra-cellular imaging and sensing *Appl Phys Lett* 99: 103701.
38. Zhang Y, Yu J, Birch DJ, Chen Y (2010) Gold nanorods for fluorescence lifetime imaging in biology. *J Biomed Opt* 15: 020504. [[Crossref](#)]
39. Cho EC, Zhang Q, Xia Y (2011) The effect of sedimentation and diffusion on cellular uptake of gold nanoparticles. *Nat Nanotechnol* 6: 385-391. [[Crossref](#)]
40. Tjelle TE, Brech A, Juvet LK, Griffiths G, Berg T (1996) Isolation and characterization of early endosomes, late endosomes and terminal lysosomes: their role in protein degradation. *J Cell Sci* 109: 2905-2914. [[Crossref](#)]
41. Zhang Y, Dan X, Li W, Yu J, Chen Y (2012) Effect of Size, Shape, and Surface Modification on Cytotoxicity of Gold Nanoparticles to Human HEP-2 and Canine MDCK Cells *J Nanomater.*
42. Jung G, Werner M, Schneider M (2008) Efficient photoconversion distorts the fluorescence lifetime of GFP in confocal microscopy: a model kinetic study on mutant Thr203Val. *Chem Phys Chem* 9: 1867-1874. [[Crossref](#)]
43. Broussard JA, Rappaz B, Webb DJ, Brown CM (2013) Fluorescence resonance energy transfer microscopy as demonstrated by measuring the activation of the serine/threonine kinase Akt. *Nat Protoc* 8: 265-281. [[Crossref](#)]
44. Lesniak A, Salvati A, Santos-Martinez MJ, Radomski MW, Dawson KA, et al., (2013) Nanoparticle Adhesion to the Cell Membrane and Its Effect on Nanoparticle Uptake Efficiency. *JA Chem Soc* 135: 1438-1444. [[Crossref](#)]
45. Ma X, Wu Y, Jin S, Tian Y, Zhang X, et al., (2011) Gold nanoparticles induce autophagosome accumulation through size-dependent nanoparticles uptake and lysosome impairment. *ACS Nano* 5: 8629-8639.
46. Peetla C, Jin S, Weimer J, Elegbede A, Labhasetwar V (2014) Biomechanics and Thermodynamics of Nanoparticle Interactions with Plasma and Endosomal Membrane Lipids in Cellular Uptake and Endosomal Escape. *Langmuir* 30: 7522-7532. [[Crossref](#)]
47. Dalal C, Saha A, Jana NR (2016) Nanoparticle Multivalency Directed Shifting of Cellular Uptake Mechanism. *J Phys Chem C* 120: 6778-6786.
48. Herd H, Daum N, Jones AT, Huwer H, Ghandehari H, et al., (2013) Nanoparticle Geometry and Surface Orientation Influence Mode of Cellular Uptake. *ACS Nano* 7: 1961-1973. [[Crossref](#)]
49. Dasgupta S, Auth T, Gompper G, (2014) Shape and Orientation Matter for the Cellular Uptake of Nonspherical Particles. *Nano Lett* 14: 687-693. [[Crossref](#)]